

# Design of Flexible Parasitic Element Patch Antenna for Biomedical Application

Ketavath Kumar Naik\*, Seelam C. S. Teja, B. V. S. Sailaja, and P. A. Vijaya Sri

**Abstract**—This paper presents the design of flexible parasitic element patch (FPEP) antenna with defects on ground plane at ISM band for biomedical application. The antenna resonates at 2.46 GHz frequency with reflection coefficient of  $-16.8$  dB in free space and at 2.45 GHz frequency when being placed on cotton and the single layer skin tissue of human body. The proposed parasitic element patch antenna is used to measure the body temperature, and the specific absorption rate (SAR) of the proposed antennas is 1.0 W/kg. The measurement data with respect to reflection coefficient, and radiation pattern are presented.

## 1. INTRODUCTION

In recent years the demand of flexible implantable antennas for biomedical applications has been increased. These implantable antennas play a key role in communication systems and act as a barrier between human body and external monitoring system. Biocompatibility, miniaturization, and patient safety make the design of implantable antennas highly challenging.

To enhance the wireless link quality of body-centric wireless communication (BWCS), a multi-polarization reconfigurable circular antenna [1], with a four-dipole radiator has been designed. The antenna resonates from 2.2 to 3.1 GHz frequency with an impedance bandwidth of 34%. A maximum peak gain of 5.2 dBi has been observed. A double layered bow-tie antenna [2] is proposed with a miniaturization technique to increase the electrical length of the antenna with a coaxial feeding method. In [3], a center square slot is loaded to a CP implanted patch antenna for miniaturization and to enhance the impedance matching. A conformal rectangular patch antenna with a rectangular slot and split ring resonators (SRR) [4] has been designed to operate for ISM band biomedical application. The antenna operates for a frequency range of 2.41 GHz to 2.81 GHz with an impedance bandwidth 400 MHz and gain of  $-19.6$  dB. A compact folded meander line structure antenna is designed [5], to reduce the size of the antenna with a gain of  $-23.7$  dBi. To improve the antenna impedance matching and reduce the observed power inside the body, a square shape CSRR [6] and an ultra-low profile dual band antenna [7] have been introduced to operate the antenna for biomedical telemetry application.

The irregular shapes of the patches provide irregularity in current distribution over the radiating patch, which produces limited polarization and asymmetry in radiation patterns compared to general rectangular patch antennas. A circular ring patch antenna [8] was designed to obtain circular polarization. To enhance the bandwidth of the antenna, a double element ring slot antenna has been designed [9]. This antenna resonates for the frequency band from 4.25 to 12.5 GHz frequency. In [10], the study of directional, omnidirectional and pattern radiation characteristics has been carried out by playing the antenna on or in close proximity to the human body. Similarly, a hexagonal shape patch antenna [11], with CPW feed has been designed for ISM band application.

---

*Received 4 March 2020, Accepted 9 July 2020, Scheduled 20 July 2020*

\* Corresponding author: Ketavath Kumar Naik (drkumarkn@hotmail.com).

The authors are with the Department of Electronics and Communication Engineering, KLEF, Vaddesaram, Guntur 522502, India.

From the literature survey, various antenna designs have been proposed to operate the antenna for WBAN application. A coplanar waveguide fed antenna [12] has been designed for in-body WBAN system applications. A split-triangle shaped flexible patch antenna [13] has been designed for WiMAX application. In [13], an antenna resonates at 3.55 GHz frequency with return loss  $-24.45$  dB. A folded UWB antenna [14] is designed for WBAN applications showing a low SAR and a truncated structure suitable for on-body applications. A conformal metamaterial antenna with  $2 \times 2$  array of H-shape unit cell [15] has been designed for an antenna to operate for WBAN communication. The antenna resonates for two frequency bands, 3–2 GHz to 3.5 GHz and 3.9 GHz to 4.3 GHz, with max gains of 4.54 dBi and 4.71 dBi. A swastika shape slot [16] and compact rectangular patch antenna [17] has been designed for an on-body application in WBAN applications.

The variation in the thickness of the human body includes effects on the implantable antennas. The dielectric properties of biological tissues: III parametric models for the dielectric spectrum of tissues as a function of frequency are listed in [18]. In [19], the effect of an antenna implanted on the human body and propagation loss in the link between an external antenna and the antenna implanted inside the human body has been studied.

In this paper, a flexible parasitic element patch (FPEP) antenna with defects on the ground plane has been designed for biomedical application. Hexagonal shape slots are considered on the ground plane to operate the antenna at ISM frequency band. The antenna analysis is carried out in free space and on cotton fabric and single layer skin tissue of the human body. The antenna resonates at 2.46 GHz in free space and 2.45 GHz frequency when being placed on the cotton-skin layer. The SAR value of 1.0 W/kg is observed at 2.45 GHz frequency.

## 2. ANTENNA DESIGN

The geometry model of the flexible parasitic element patch (FPEP) antenna is proposed for the on-body application, shown in Fig. 1. A kapton polyimide substrate material, with  $(\epsilon_r)$ 3.5, loss tangent  $(\delta)$ 0.004, is considered as a substrate material.  $L_1$  and  $W_1$  are considered as the length and width of the substrate material with a height of 0.07 mm. Rectangular shape parasitic elements are considered as radiating elements and are coated on the substrate material with a thickness of 0.01 mm as shown in Fig. 1(a). The other side of the substrate material is coated with ground plane. Two hexagonal shape ring slots with radii  $r_1$ ,  $r_2$ ,  $r_3$ , and  $r_4$  are etched from the ground plane as shown in Fig. 1(b). The optimized

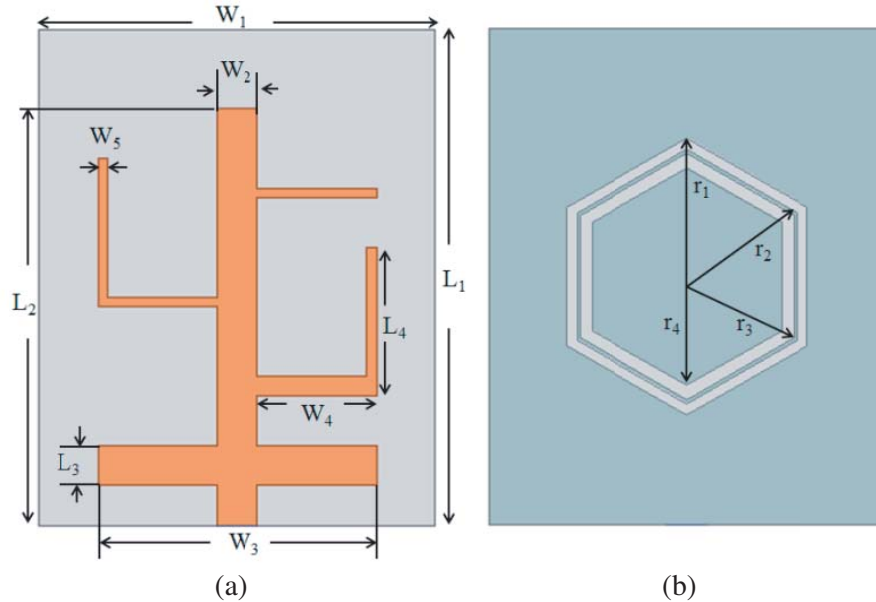


**Figure 1.** Geometry of the proposed FPEP antenna. (a) Radiating patch. (b) Ground plane.

parameters of the proposed antennas, parasitic length and widths, are as follows:  $L_1 = 25$ ,  $L_2 = 21$ ,  $L_3 = 2$ ,  $L_4 = 7$ ,  $W_1 = 20$ ,  $W_2 = 2$ ,  $W_3 = 14$ ,  $W_4 = 6$ ,  $W_5 = 0.5$ ,  $r_1 = 7$ ,  $r_2 = 6.4$ ,  $r_3 = 6.2$ ,  $r_4 = 5.5$  (all the measurement units in millimetres).

The proposed FPEP antenna model is tested in free space and on the skin layer tissue of the human body with a cotton material between the antenna and skin tissue. Fig. 2 shows the geometry of the antenna placed on the cotton layer with 1 mm height and skin layer with 1.6 mm height. The dielectric properties of the cotton and skin layer are listed in Table 1.

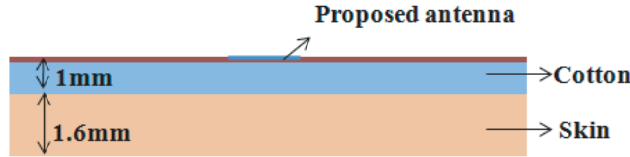


Figure 2. Geometry of proposed antenna on cotton layer and ground plane.

Table 1. Dielectric properties of skin and cotton at 2.45 GHz frequency.

Material	dielectric constant ( $\epsilon_r$ )	loss tangent (S/m)
Skin	42.923	0.27253
cotton	1.6	0.04

### 3. EVOLUTION PROCESS OF FPEP

The evolution process of the FPEP antenna model is shown in Fig. 3. In the first step of the design (Ant-1), a monopole rectangular strip patch antenna with full ground is considered. Ant 1 does not

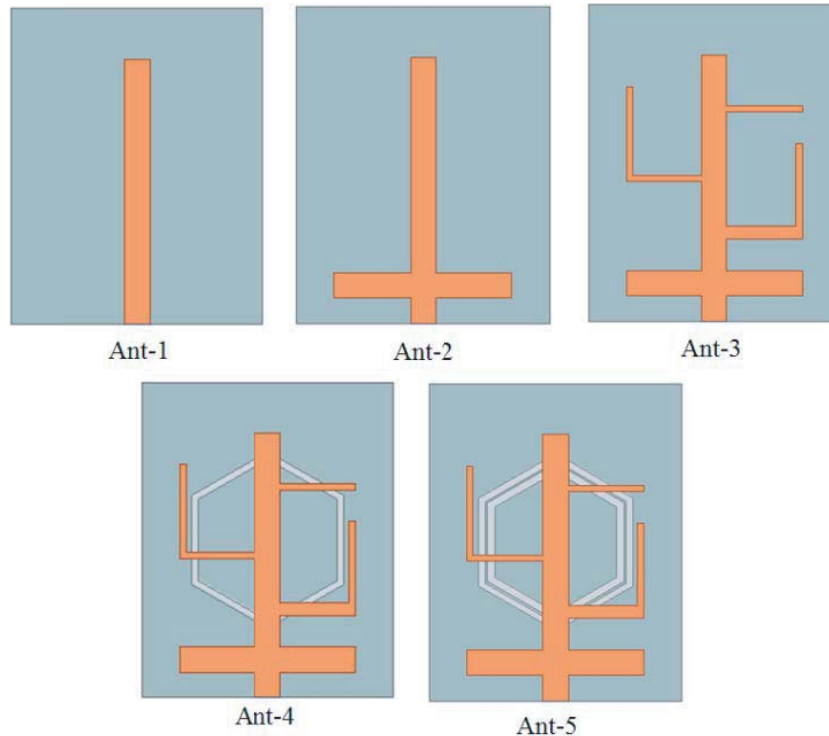
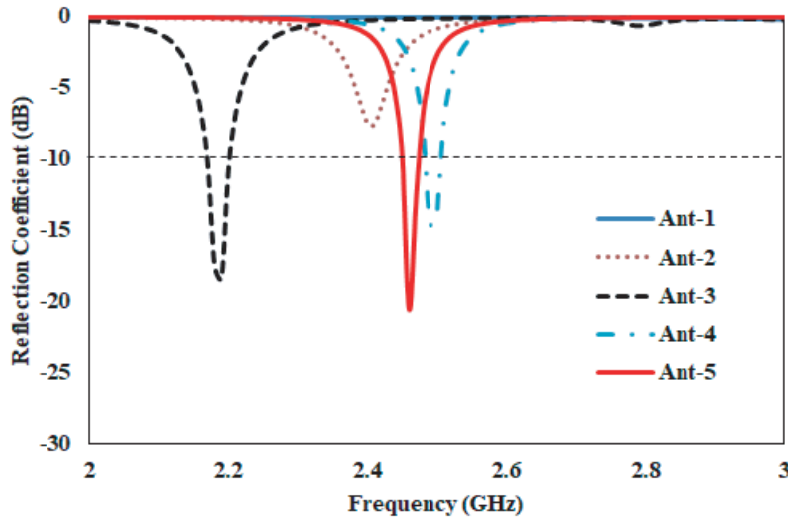


Figure 3. The evolution process of FPEP antenna.

show any resonance. As the antenna is intended for ISM application, Ant-2 is designed by adding a horizontal rectangular strip to Ant-1. In this step, the antenna resonates at 2.4 GHz with a reflection coefficient of  $-7.4$  dB.

Further in the evolution process (Ant 3), a set of stubs are added to the parasitic element. In this step, the antenna resonates at 2.28 GHz frequency with  $-20.02$  dB reflection coefficient. For better current path of the FPEP antenna (Ant 3), hexagonal ring slots are considered. Ant 4 is designed with a hexagonal slot on ground plane, and the antenna operates at 2.49 GHz frequency with reflection coefficient  $-14.54$  dB. The final step of the evolution process is designed by adding two hexagonal ring slots to the ground plane of FPEP. Ant 5 resonates at 2.46 GHz with  $-20.58$  dB reflection coefficient. The reflection coefficient plot for the evolution process of FPEP antenna is shown in Fig. 4.

The parametric analysis for the proposed FPEP antenna is also carried out by varying dimensions of  $L_3$  and  $W_3$ , respectively. Fig. 5 and Fig. 6 show the analysis of antenna by varying  $L_3$  and  $W_3$  as 1 mm, 2 mm, and 3 mm. From the plot the width of  $L_3$  and  $W_3$  with 2 mm shows good result when compared to 1 mm and 3 mm, respectively. The variations with respect to frequency and reflection coefficient by varying  $L_3$  and  $W_3$  are tabulated in Table 2.



**Figure 4.** Evolution process of proposed antenna.

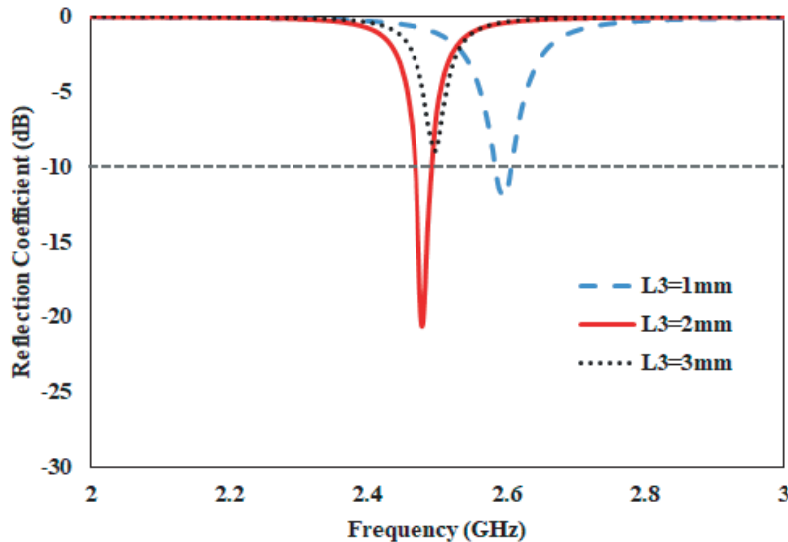


**Figure 5.** Parametric analysis of FPEP antenna by varying  $L_3$ .

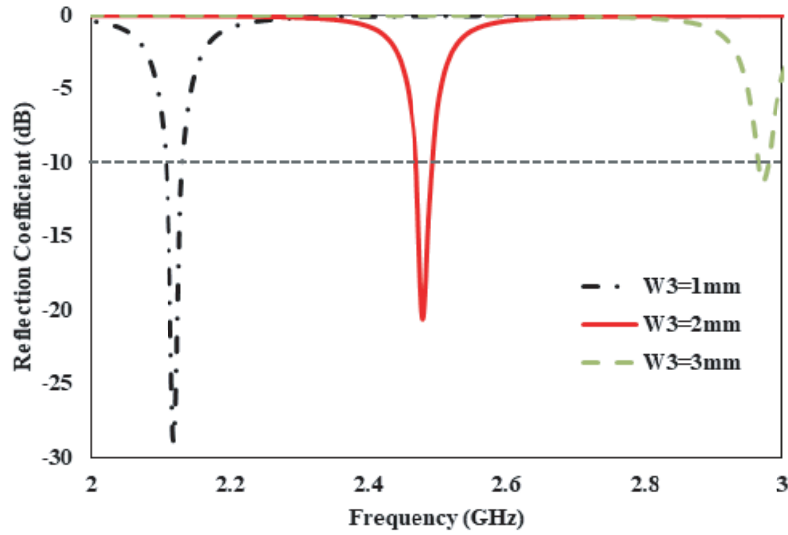


Figure 6. Parametric analysis of FPEP antenna by varying  $W_3$ .

Table 2. Parametric analysis of FPEP antenna by varying  $L_3$  and  $W_3$ .

Parameter	Operating Frequency (GHz)	Reflection Coefficient (dB)
$L_3 = 1 \text{ mm}$	2.59	-11.41
$L_3 = 2 \text{ mm}$	2.46	-20.58
$L_3 = 3 \text{ mm}$	2.5	-8.92
$W_3 = 1 \text{ mm}$	2.12	-28.8
$W_3 = 2 \text{ mm}$	2.46	-20.58
$W_3 = 3 \text{ mm}$	2.97	-11.32

#### 4. RESULTS AND DISCUSSION

The antenna is designed and analyzed using Ansys HFSS tool. Fig. 7 represents the simulated and measured reflection coefficients of the proposed antenna model in free space and on the skin-cotton layer. The variation in the simulated and measured reflection coefficients is due to the parasitic effect and fabrication error of the proposed antenna.

The proposed antenna resonates at 2.46 GHz frequency with reflection coefficient  $-20.58 \text{ dB}$  in simulation and 2.45 GHz frequency with reflection coefficient  $-25.7 \text{ dB}$  in 1 measurement. In simulation and measurement the antenna placed on the skin layer resonates at 2.45 GHz frequency. The designed antenna is used to measure the body temperature. The measurement setup of proposed antenna with

Table 3. Comparison of proposed antenna with simulated and measured.

	Validation	Operating Frequency (GHz)	Reflection Coefficient (dB)	Bandwidth (GHz)
Simulated	Free space	2.46	-20.58	2.45–2.48
	Skin-cotton	2.45	-12.28	2.44–2.47
Measured	Free space	2.45	-25.71	2.40–2.51
	Skin-cotton	2.44	-16.35	2.43–2.48

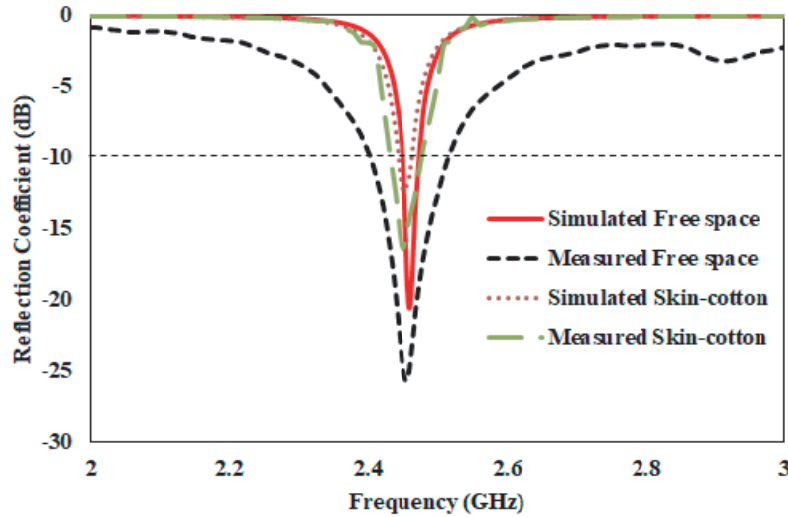


**Figure 7.** Reflection coefficient of the FPEP antenna.



**Figure 8.** Photograph of measuring the reflection coefficient with Network analyser.

network analyser is shown in Fig. 8. The prototype of proposed antenna is shown in Fig. 9. The experimental setup of the antenna in an anechoic chamber is shown in Fig. 10. The comparison of simulated and measured results for the proposed FPEP antenna model is tabulated in Table 3.

The 3D-gain plot of antenna at 2.46 GHz frequency is shown in Fig. 11. From the figure a minimum gain of  $-1.84$  dB is observed. The radiation plot for the FPEP antenna at 2.46 GHz frequency is shown in Fig. 12. A bi-directional radiation pattern with major radiation at  $33^\circ$  and  $21^\circ$  angles is observed, and 10 dB isolation is seen between co-polarization and cross-polarization.

The surface current distribution for the FPEP antenna is shown in Fig. 13. The maximum current distribution of 2.423 A/m is shown at 2.46 GHz frequency.

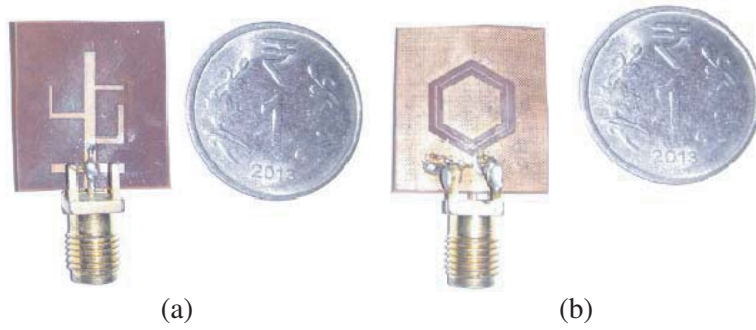


Figure 9. Prototype of FPEP antenna. (a) Radiating patch and (b) Ground plane.

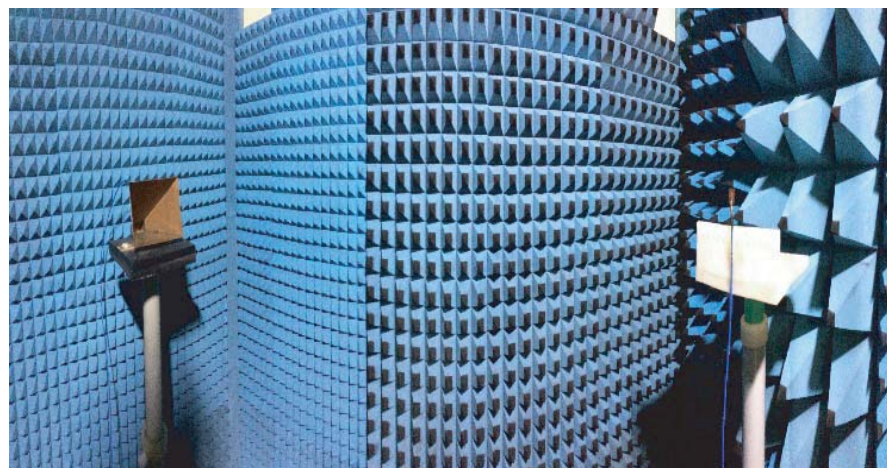


Figure 10. Anechoic chamber facility for measurement.

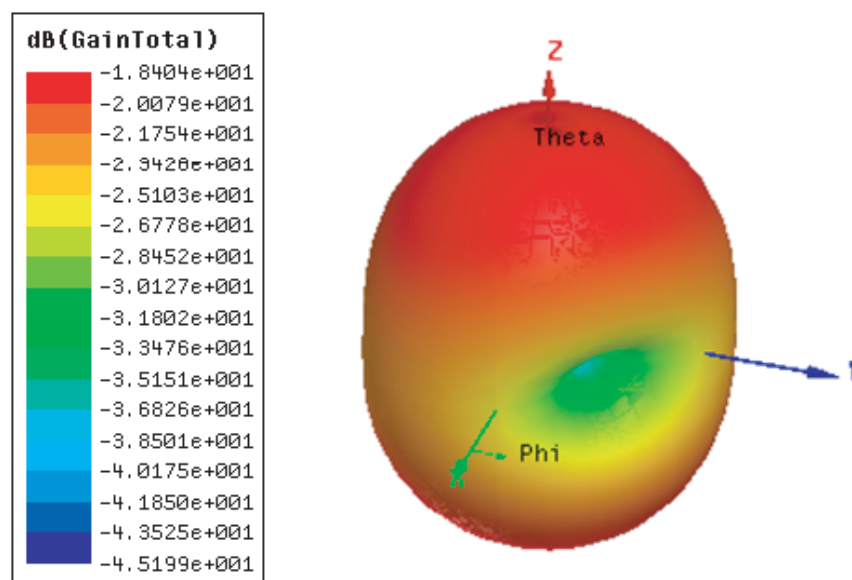
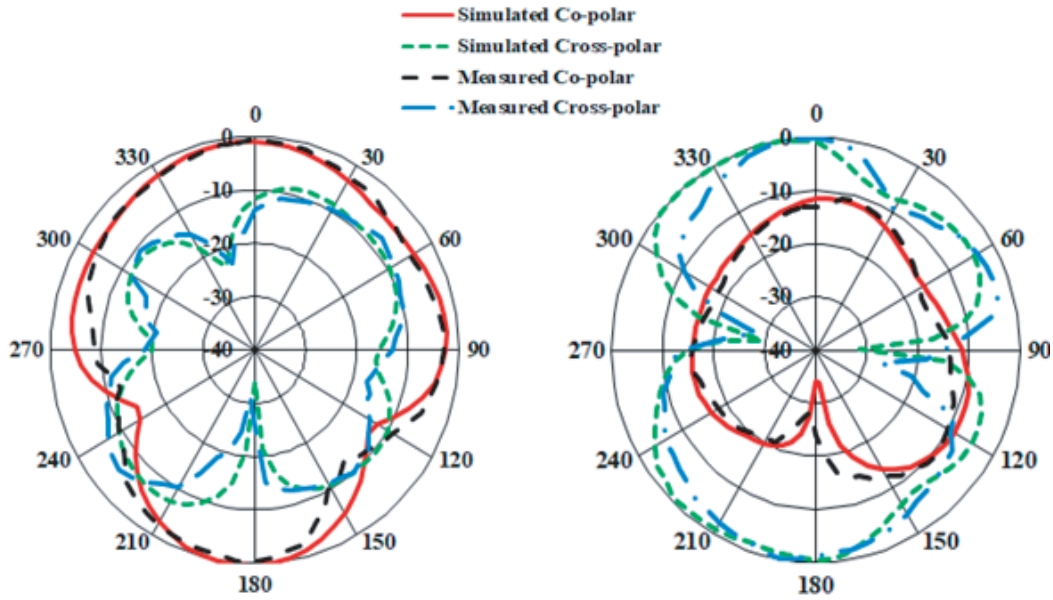


Figure 11. Gain plot of the proposed FPEP antenna.



**Figure 12.** Radiation pattern of the proposed FPEP antenna at 2.46 GHz frequency. (a) *E*-plane. (b) *H*-plane.

The SAR value of the proposed antenna on the skin layer tissue is shown in Fig. 14 with the minimum value of 1.0 W/kg which is less than 1.6 W/kg as per IEEE standards. The comparison of the proposed antenna with the previous antenna models is tabulated in Table 4.

**Table 4.** Comparison of proposed FPEP antenna with the previous models.

Ref. No.	Antenna Size	Material	Operating Bandwidth	Application
[3]	$10 \times 10 \times 1.27 \text{ mm}^3$	Rogers 3010	2.4 to 2.48 GHz	ISM Band
[4]	$24 \times 22 \times 0.07 \text{ mm}^3$	Polyimide	2.01 to 2.82 GHz	ISM Band
[6]	$15 \times 30 \text{ mm}^2$	-	401 to 406 MHz 433.1 to 434.8 MHz 868.0 to 868.8 MHz 902.8 to 928.0 MHz 2.45 GHz	MedRadio and ISM
[10]	$25 \times 35 \text{ mm}^2$	FR-4	UW	On-Body Application
[11]	$43 \times 28 \times 1.6 \text{ mm}^3$	FR-4	2.27–2.57 GHz	ISM band
[15]	$42 \times 62 \text{ mm}^2$	RT-Duroid 5880	3.2 to 3.5 GHz 3.9 to 4.3 GHz	On-Body WBAN Communication
[16]	$27 \times 27 \times 1 \text{ mm}^3$	FR-4	4.25 to 12.5 GHz (SS-UWB)	On-Body Application
[17]	$62 \times 43 \times 1.67 \text{ mm}^3$	FR-4	2.3369–2.443 GHz	WBAN
Proposed antenna	$25 \times 20 \times 0.07 \text{ mm}^3$	Polyimide	2.45 to 2.48 GHz	ISM Band

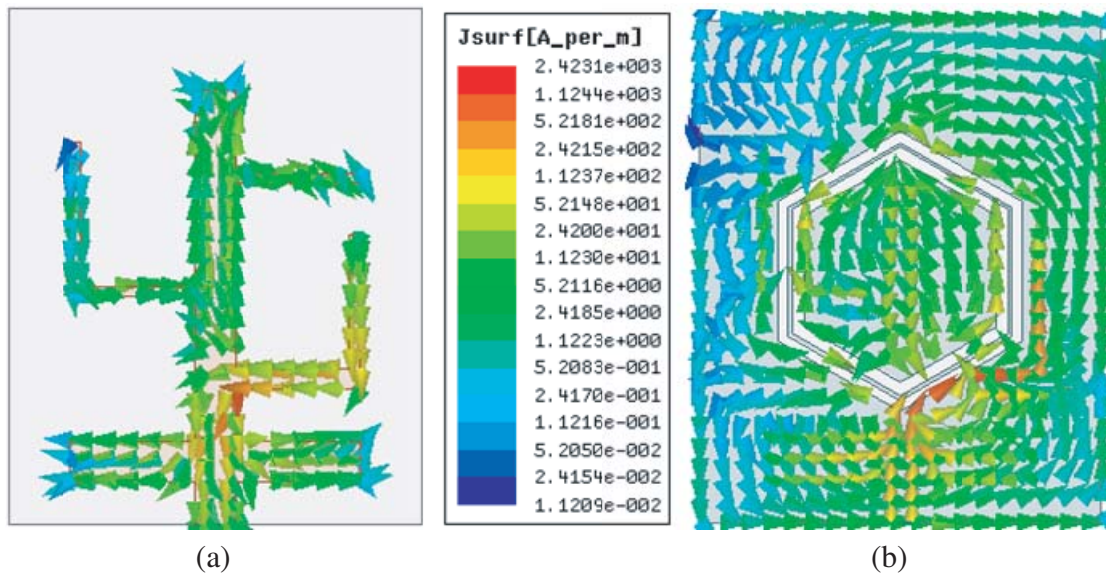


**Figure 13.** Surface current distribution of FPEP antenna at 2.46 GHz frequency, (a) radiating patch and (b) ground plane.

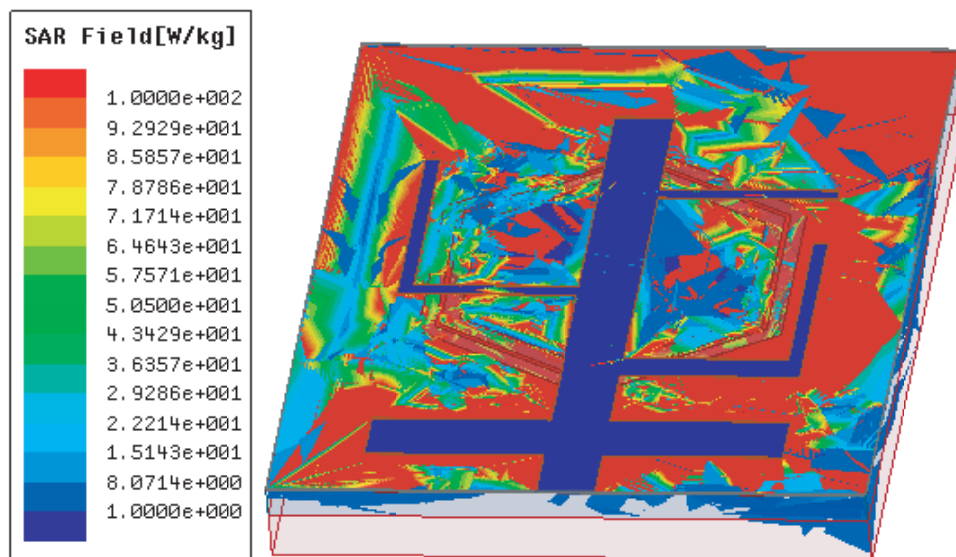


**Figure 14.** SAR of the proposed antenna on skin-cotton layer.

## 5. CONCLUSION

In this paper, we have designed and tested an ISM antenna for the on-body application. The antenna is a parasitic structure with hexagonal ring in the ground plane. The designed antenna operates at 2.46 GHz, and measurement result shows the resonance at 2.45 GHz. The proposed antenna is used to measure the body temperature. This proves the agreement between the experimental and simulated results. The radiation pattern is bi-directional, and a 10 dB isolation is observed between co-polarization and cross-polarization.

## ACKNOWLEDGMENT

This work is supported by Department of Science and Technology (DST), SERB Govt. of India. (File No.: EEQ/2016/000754).

## REFERENCES

1. Wong, H., W. Lin, L. Huitema, and E. Arnaud, "Multi-polarization reconfigurable Antenna for Wireless Biomedical System," *IEEE Trans. on Biomed. Circuits Syst.*, Vol. 11, No. 3, 652–660, Jun. 2017.
2. Li, X., M. Jalivand, Y. Sit, and T. Zwick, "A compact double-layer on-body matched bowtie antenna for medical diagnostics," *IEEE Trans. on Antenna and Propag.*, Vol. 62, No. 4, 1808–1816, Apr. 2014.
3. Liu, C., Y.-X. Guo, and S. Xiao, "Capacitively loaded circularly polarized implantable patch antenna for ISM band biomedical applications," *IEEE Trans. on Antenna and Propag.*, Vol. 62, No. 5, 2407–2417, May 2104.
4. Ketavath, K. N., D. Gopi, and S. Sandhya Rani, "In-vitro test of miniaturized CPW-fed implantable conformal patch antenna at ISM band for biomedical applications," *IEEE Access*, Vol. 7, 43547–43554, 2019.
5. Lesnik, R., N. Verhovski, I. Mizrachi, B. Milgrom, and M. Haridim, "Gain enhancement of a compact implantable dipole for biomedical applications," *IEEE Antennas and Wireless Propagation Letters*, Vol. 17, No. 10, 1778–1782, Aug. 2018.
6. Alrawashdeh, R. S., Y. Huang, M. Kod, and A. A. B. Sajak, "A broadband flexible implantable loop antenna with complementary split ring resonator," *IEEE Antennas and Wireless Propagation Letters*, Vol. 14, 1506–1509, 2015.
7. Raad, H. K., H. M. Al-Rizzo, A. Isaac, and A. I. Hammoodi, "A compact dual band polyimide based antenna for wearable and flexible telemedicine devices," *Progress In Electromagnetics Research C*, Vol. 63, 153–161, 2016.
8. Bao, X. L. and M. j. Ammann, "Compact annular-ring embedded circular patch antenna with cross-slot ground plane for circular polarization," *Electronics Lett.*, Vol. 42, No. 4, Feb. 2006.
9. Behdad N. and K. Sarabandi, "Wideband double-element ring slot antenna," *Electronics Lett.*, Vol. 40, No. 7, Apr. 2004.
10. Terence, S., P. See, and Z. N. Chen, "Experimental characterization of UWB antennas for on-body communication," *IEEE Trans. on Antenna and Propag.*, Vol. 57, No. 4, 866–874, Apr. 2009.
11. Abdulhasan, R. A., R. Alias, and K. N. Ramli, "A compact CPW fed UWB antenna with quad band notch characteristics for ISM band applications," *Progress In Electromagnetics Research M*, Vol. 62, 79–88, 2017.
12. Kurup, D., M. Scarpello, G. Vermeeren, W. Joseph, K. Dhaenens, F. Axisa, L. Martens, D. V. Ginste, H. Rogier, and J. Vanfleteren, "In-body patch loss models for implants in heterogeneous human tissues using implantable slot dipole conformal flexible antennas," *EURASIP Journal on Wireless Commun. and Networking*, Article number: 51 (2011), 2011.
13. Naik, K. K. and D. Gopi, "Flexible CPW-fed split-triangular shaped patch antenna for WIMAX application," *Progress In Electromagnetics Research M*, Vol. 70, 157–166, 2018.
14. Kang, C. H., S. J. Wu, and J. H. Tarnq, "A novel folded UWB antenna for wireless body area network," *IEEE Trans. on Antenna and Propag.*, Vol. 60, No. 2, 1139–1142, Feb. 2012.
15. Hazanka, B., B. Basu, and J. Kumar, "A multi-layered dual-band on-body conformal integrated antenna for WBAN communication," *International Journal of Electronics and Communications*, Vol. 95, 226–235, Oct. 2018.
16. Kumar, V. and B. Gupta, "On-body measurements of SS-UWB patch antenna for WBAN applications," *International Journal of Electronics and Communications*, Vol. 70, No. 5, 668–675, May 2016.

17. Ali, S. M., V. Jeoti, T. Saeidi, and W. P. Wen, "Design of compact microstrip patch antenna for WBAN applications at ISM 2.4 GHz," *Indonesian Journal of Electrical Engineering and Computer Science*, Vol. 15, No. 3, 1509–1516, Sept. 2019.
18. Gabriel, C., *Compilation of the Dielectric Properties of Body Tissues at RF and Microwave Frequencies*, King's College, London, UK, 1996.
19. Gemio, J., J. Parron, and J. Soler, "Human body effects on implantable antennas for ISM bands applications: Models comparison and propagation losses study," *Progress In Electromagnetics Research*, Vol. 110, 437–452, 2010.